Protonated Carboxyl Anchor for Stable Adsorption of Ru N749 Dye (Black Dye) on a TiO2 Anatase (101) Surface

ARTICLE *in* JOURNAL OF PHYSICAL CHEMISTRY LETTERS · JANUARY 2012

Impact Factor: 7.46 · DOI: 10.1021/jz201583n

8 AUTHORS, INCLUDING:

Keitaro Sodeyama
Kyoto University
41 PUBLICATIONS **437** CITATIONS
SEE PROFILE

Masato Sumita
National Institute for Materials Science
35 PUBLICATIONS **312** CITATIONS
SEE PROFILE

Conn O'Rourke
University of Bath
5 PUBLICATIONS **62** CITATIONS
SEE PROFILE

David R Bowler
University College London
161 PUBLICATIONS **3,789** CITATIONS
SEE PROFILE

THE JOURNAL OF PHYSICAL CHEMISTRY Letters

Letter

pubs.acs.org/JPCL

Protonated Carboxyl Anchor for Stable Adsorption of Ru N749 Dye (Black Dye) on a TiO_2 Anatase (101) Surface

Keitaro Sodeyama,[†,‡] Masato Sumita,[†] Conn O'Rourke,[†,§,∥] Umberto Terranova,[†,§,∥] Ashraful Islam,[‡,⊥] Liyuan Han,[‡,⊥] David R. Bowler,[†,§,∥] and Yoshitaka Tateyama*[,†,‡,#]

[†]International Center for Materials Nanoarchitectonics (WPI-MANA), National Institute for Materials Science (NIMS), 1-1 Namiki, Tsukuba, Ibaraki 305-0044, Japan

[‡]CREST and [#]PRESTO, Japan Science and Technology Agency (JST), 4-1-8 Honcho, Kawaguchi, Saitama 333-0012, Japan

[§]Department of Physics and Astronomy, University College London, Gower Street, London WC1E 6BT, U.K.

[∥]London Centre for Nanotechnology, 17-19 Gordon Street, London WC1H 0AH, U.K.

[⊥]Photovoltaic Materials Unit, National Institute for Materials Science (NIMS), 1-2-1 Sengen, Tsukuba, Ibaraki 305-0047, Japan

Supporting Information

ABSTRACT: We have investigated the adsorption stability of ruthenium N749 dye [black dye (BD)], a highly efficient dye for dye-sensitized solar cells (DSCs), through protonated and deprotonated carboxyl group anchors on a TiO_2 anatase (101) surface by using first-principles calculations. Geometry optimizations of the surface system with a supercell and the UV−visible spectrum calculation of the optimized dye structure were carried out. Among the configurations with one and two anchors, the BD adsorption anchored with one protonated carboxyl group was found to be the most stable, in contrast to most previous reports. Hydrogen bonding between the proton retained in BD and the surface oxygen is responsible for the stability of the protonated anchor. We confirmed that the calculated UV−visible spectrum of the most stable dye structure shows the best consistency with the experimental data. It is also demonstrated that the electronic density of states largely depends on the proton position. This novel aspect of adsorption via a protonated carboxyl anchor gives a new perspective for interfacial electronic processes of DSCs.

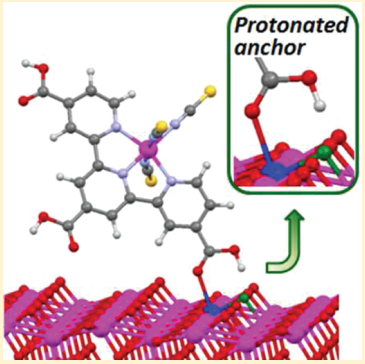

SECTION: Surfaces, Interfaces, Catalysis

Dye-sensitized solar cells (DSCs) are being developed as inexpensive solar-to-electricity conversion devices, compared to the conventional Si-based solar cells.[1−3] Many DSC systems have been developed so far for applications. Among them, the systems with Ru(II) polypyridyl dyes usually give high efficienies.[1−7] The most typical are N3 and N719 dyes (doubly deprotonated form of N3 dye).[4,5] In order to improve the efficiency, N749 dye [Ru(4,4′,4″-tricarboxy-2,2′:6′,2″-terpyridine)$(NCS)_3$], so-called black dye (Scheme 1a), was synthesized subsequently[6] by introducing one terpyridine and more thiocyanate (NCS) ligands instead of two bipyridine ones in the N3/N719 dyes to increase the absorption in the near-IR region. However, the resulting efficiencies were still low, and improvement based on the atomistic understanding is crucial for further breakthroughs. In this respect, microscopic examinations of Ru dye systems are of great importance. These systems are also useful to understand the general properties of DSC systems because they involve typical features of DSCs, such as organometallic complexes and adsorption via polypyridyl ligands to the surface. Although the DSC conversion efficiency is controlled by many factors,[3,4,8−10] the alignment of the excited electron level (LUMO) of the dye and the conduction band minimum (CBM) of the TiO_2 surface is crucial for the interfacial charge transfer. Because this alignment is affected by the adsorption manner,[11,12] the adsorption structure of the dye is still an essential property, especially for the initial electron injection to the TiO_2 surface.[13,14]

Upon adsorption of Ru dyes on the TiO_2 anatase (101) surface, carboxyl groups in the polypyridyl ligands act as anchors to five-fold-coordinated Ti (Ti_{5c}) sites on the surface.[15−17] For N3/N719 dyes, the adsorption with two deprotonated carboxyl group (namely carboxylate group) anchors has been regarded as being most probable.[5,18−22] However, recent first-principles studies revised this scenario, indicating that three-anchor adsorption with one bidentate bridging and two monodentates is more stable,[12,23] where the one carboxylate (deprotonated) group has a hydrogen bond (HB) to the surface proton bound to a two-fold-coordinated oxygen (O_{2c}). Hence, the adsorption mode and the number of anchors are still under investigation. The protonation/deprotonation of the carboxyl anchors is also controversial (Scheme 1b−e). Conventionally, the deprotonated anchor is

Received: December 1, 2011
Accepted: January 24, 2012

   dx.doi.org/10.1021/jz201583n | J. Phys. Chem.Lett. 2012, 3, 472−477

Scheme 1. Schematic Structure of Black Dye and Representations of Possible Adsorption Modes[a]

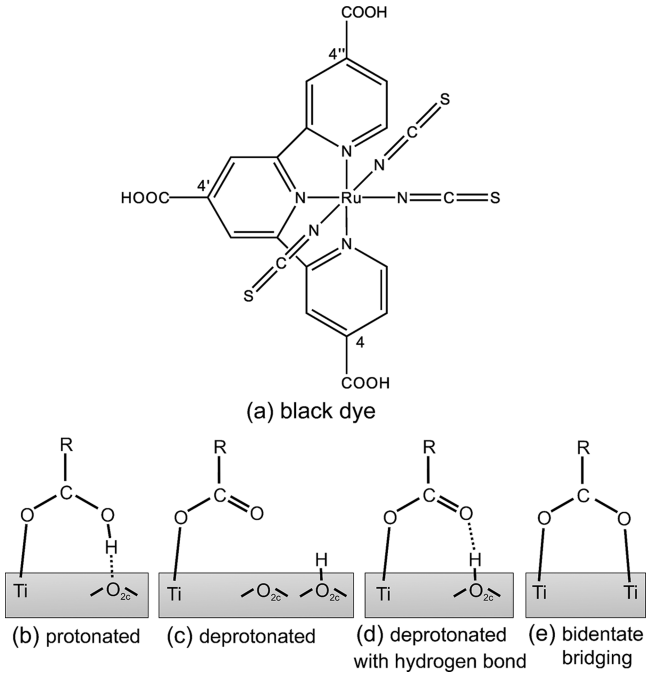

[a](a) Structure of fully protonated Ru N749 dye (black dye). (b) A protonated carboxyl anchor to a surface Ti site; the proton stays in the carboxyl group and forms hydrogen bond to O_{2c}. (c) A deprotonated carboxyl (carboxylate) anchor without hydrogen bond; transferred proton of the carboxyl group adsorbs at the O_{2c} site far away from the anchor. (d) A deprotonated carboxylate anchor; the proton adsorbs at the O_{2c} and forms a hydrogen bond to the oxygen atom of carboxylate group. (e) A bidentate bridging carboxylate anchor.

regarded as being more stable than the protonated anchor. However, in the adsorptions of formic acid and glycine to the TiO_2 anatase (101) surface, protonated anchor adsorptions are suggested to be more stable.[24,25] As already pointed out, the adsorption mode as well as the proton position affects the electronic states of the dye/TiO_2 interface, such as the conduction band position of the TiO_2 surface, the photoabsorption spectra of the dye itself,[19−21] and the electron injection efficiency.[13,14] Therefore, detailed investigation of the protonation/deprotonation of dye carboxyl anchors is still important.

In this Letter, we investigate the adsorption stability of Ru N749 dye (black dye) on the TiO_2 anatase (101) surface, with emphasis on the protonation and deprotonation of the carboxyl group anchors as well as the number of anchors. To our knowledge, there is no first-principles study on the black dye adsorption on the TiO_2(101) surface. We carry out density functional theory (DFT)[26] based geometry optimization of the dye/TiO_2 systems. The supercell approach[26] with periodic boundary conditions and a plane wave basis set are used to avoid any artifacts of cluster models for the surface. Due to the stiffness of the terpyridine ligand, only one- and two-anchor adsorption modes are considered. We determine the most stable adsorption mode by comparing the relative total energies and examine the origin of the stability with structural analysis. In order to verify the present stability, we compare the calculated UV−visible spectra of the optimized dye structures with the experimental data. In this analysis, a time-dependent

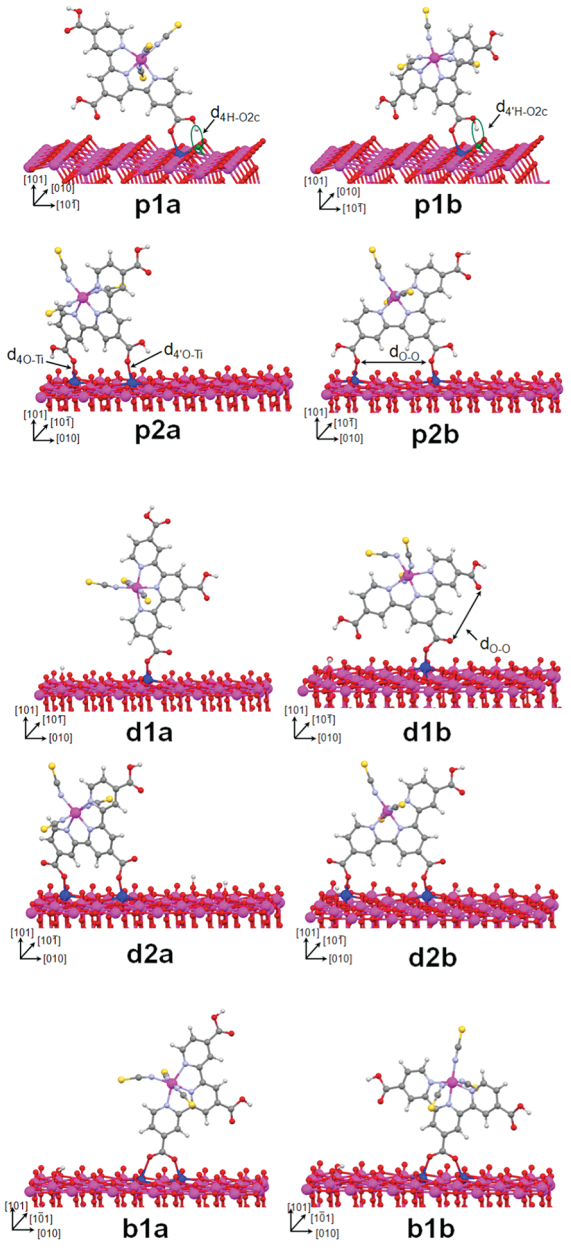

Figure 1. Optimized adsorbed structures of black dye on the TiO_2 anatase (101) surface. Protonated adsorptions with one and two protonated anchors are labeled as **p1x** and **p2x**, respectively (**x** = **a**,**b**), while **d1x** and **d2x** (**x** = **a**,**b**) indicate the structures with deprotonated one and two anchors, respectively. **b1x** (**x** = **a**,**b**) indicates the bidentate bridging adsorptions with one anchor.

DFT (TDDFT) linear response scheme[27] is used with the conductor-like polarized continuum model (CPCM) to take the effect of typically used acetonitrile solvent into account. We show the projected density of states (PDOS) to illustrate the differences between protonation and deprotonation. The geometry optimizations and PDOS calculations are performed in vacuo as the first step, although DSCs are working under an electrolyte solution environment.[1−3] Detailed calculation conditions are described in the Computational Details section.

Concerning the structure models, we focus on the number of carboxyl group anchors (label ***n***), and their protonation or deprotonation (label **p** or **d**). In each category, there are two types of the adsorption modes depending on the dye

dx.doi.org/10.1021/jz201583n | J. Phys. Chem.Lett. 2012, 3, 472−477

Table 1. Relative Energies ΔE (eV) with Respect to the p1a Structure and Specific Interatomic Distances (Å) of Adsorbed Structures of Black Dye on the Anatase (101) Surface in Protonated, Deprotonated, and Bidentate Bridging Forms[a]

	protonated				deprotonated				bidentate bridging		desorbed
	one anchor (**p1x**)		two anchor (**p2x**)		one anchor (**d1x**)		two anchor (**d2x**)		one anchor (**b1x**)		
figure	**p1a**	**p1b**	**p2a**	**p2b**	**d1a**	**d1b**	**d2a**	**d2b**	**b1a**	**b1b**	
ΔE	0.00	0.12	0.17	0.22	1.08	1.60	1.57	1.94	2.01	1.10	
d_{4H-O2c}	1.62		2.81	3.29							
$d_{4'H-O2c}$		1.61	3.16	3.30							
d_{O-O}	6.75	6.73	7.05	6.93	6.33	6.38	7.18	7.03	6.52	6.63	6.75
d_{4O-Ti}	2.36		2.21	2.11	1.94		1.94	1.92	2.27		
$d_{4'O-Ti}$		2.43	2.13	2.07		2.11	1.84	1.92		2.14	

[a]Specific bonds are illustrated in Figure 1. The d_{O-O} of **b1b** and the d_{4O-Ti} and $d_{4'O-Ti}$ of **b1x** are averaged values due to the symmetry of the **b1x** structures.

orientation on the surface (e.g., parallel or perpendicular to the [010] direction) and the positions of the carboxyl groups used for the anchors (e.g., 4, 4′, or 4″ carboxyl groups in Scheme 1a). We also examine bidentate bridging adsorption (label **b**), shown in Scheme 1e. Because large strain is expected for the two-anchor structures, we focus on two types of the one-anchor mode only. All of the investigated adsorption modes, **p1x**, **p2x**, **d1x**, **d2x**, and **b1x** (**x** = **a**,**b**), are shown in Figure 1. In the deprotonated forms, the dissociated protons are put on the O_{2c} sites on the surface, far from the anchored Ti_{5c} one.

In order to compare the total energies of different structures, we use the same numbers of atoms and species for all of the structures examined. Then, we assume that the fully protonated black dye is the initial state before adsorption. In the synthesis, Ru dye is usually introduced on the TiO_2 surface with methanol and so forth. Because the pK_a of the carboxyl group for such solvents is usually higher than that of water,[28] the proton in the carboxyl group is likely to remain bonded until adsorption at least. Sometimes, black dye is referred to as having one carboxyl group (COOH) and two carboxylate groups with TBA^+ ($-COO^-{\cdot}TBA^+$). Even in this case, the cations seem to stay in the black dye, and the present fully protonated black dye would be a reasonable model for it.

Table 1 lists the relative total energies of 10 optimized structures investigated, with respect to that of the most stable **p1a** structure. We found that the deprotonated (**d*n*x**) and bidentate bridging (**b1x**) forms are less stable than the protonated ones (**p*n*x**). This indicates that the proton affinity of the O_{2c} site on the TiO_2 anatase (101) surface is quite small compared to that for the carboxyl groups biding to Ti_{5c}. Between the **p1x** and **p2x**, the one-anchor modes are more stable than the two-anchor, indicating that the Ti−O bonding is not the sole source of the stabilization.

To understand the relative stability among the adsorption modes, we examined their structural parameters (Table 1). We found that the distance between the proton in the carboxyl group anchor and the nearby O_{2c} site in **p1x** is around 1.6 Å, clearly indicating formation of a strong HB. On the other hand, no HB appears in **p2x** structures. Therefore, the stabilities of **p1x** structures are significantly stabilized by the presence of the HB. It is also found that **p2x** structures have large strain in the terpyridine ring, based on comparison between the d_{O-O} (see Figure 1 for definition) of the adsorbed structures (6.9−7.1 Å) and that of the gas-phase one (6.75 Å), which may account for the absence of the HB and their relative instability. The Ti−O bond distances in the protonated and deprotonated structures are around 2.1−2.4 and 1.8−2.1 Å, respectively. The former is close to the Ti−O distance of molecularly adsorbed water, while the latter corresponds to the hydroxyl adsorption.[29] On the TiO_2 anatase (101) surface, molecular adsorption is energetically favored for water.

In the present deprotonated adsorption modes, the proton is adsorbed at an O_{2c} site far away from the anchoring site. Thus, this mode loses the binding energy of OH in the carboxyl group as well as the HB energy, which may lead to destabilization irrespective of the gain in the adsorption energy to the O_{2c} site. Therefore, we have also carried out geometry optimization of a deprotonated mode where the proton is put at the nearest O_{2c} to the anchoring site. We then observed that the proton moved back to the oxygen in the dye carboxylate group after the geometry optimization (Supporting Information Figure S2). This indicates that the O_{2c} site on the TiO_2 surface is more acidic (smaller pK_a) than the carboxyl anchor with the adsorption to Ti_{5c}. This is consistent with the previous first-principles free-energy calculations showing $pK_a = -1$ for the O_{2c} site in the rutile TiO_2.[30] Although the TiO_2 surface is usually regarded as being basic, we emphasize that the acidity and basicity depend on the surface local sites, and this local acidity is an important feature of adsorption on metal oxide surfaces. The proton position of the bidentate bridging modes is in the same situation as the deprotonated adsorption modes; the proton is adsorbed at an O_{2c} site far away from the anchoring site. Therefore, the bidentate bridging mode also loses the binding energy of OH in the carboxyl group and the HB energy, which induces the destabilization in comparison with the protonated modes. From the viewpoint of the experimental evidence, the instability of the deprotonated adsorption modes is consistent with the FT-IR spectra measurements,[12] and the presence of the protonated adsorption modes does not contradict with the spectra.

In order to further verify the present results, we compare the calculated UV−visible spectra of the most stable structures of the **p*n*a**, **d*n*a**, and **b1b** categories with experimental data; these are shown in Figure 2a. The experimental spectra are measured including the TiO_2 surface immersed in acetonitrile solvent. Assuming that the main features of the spectra come from the intramolecular excitations, we extract only the dye from the optimized dye/TiO_2 structures obtained within the supercell approach. Here, we also calculate the UV−visible spectrum of the most stable three-anchored adsorption structure of N719 proposed in the previous study[22] for the wavelength (energy) reference because the absolute excitation energies calculated using the B3LYP functional are still underestimated slightly. This underestimation of the excitation energy is a general

dx.doi.org/10.1021/jz201583n | J. Phys. Chem.Lett. 2012, 3, 472−477

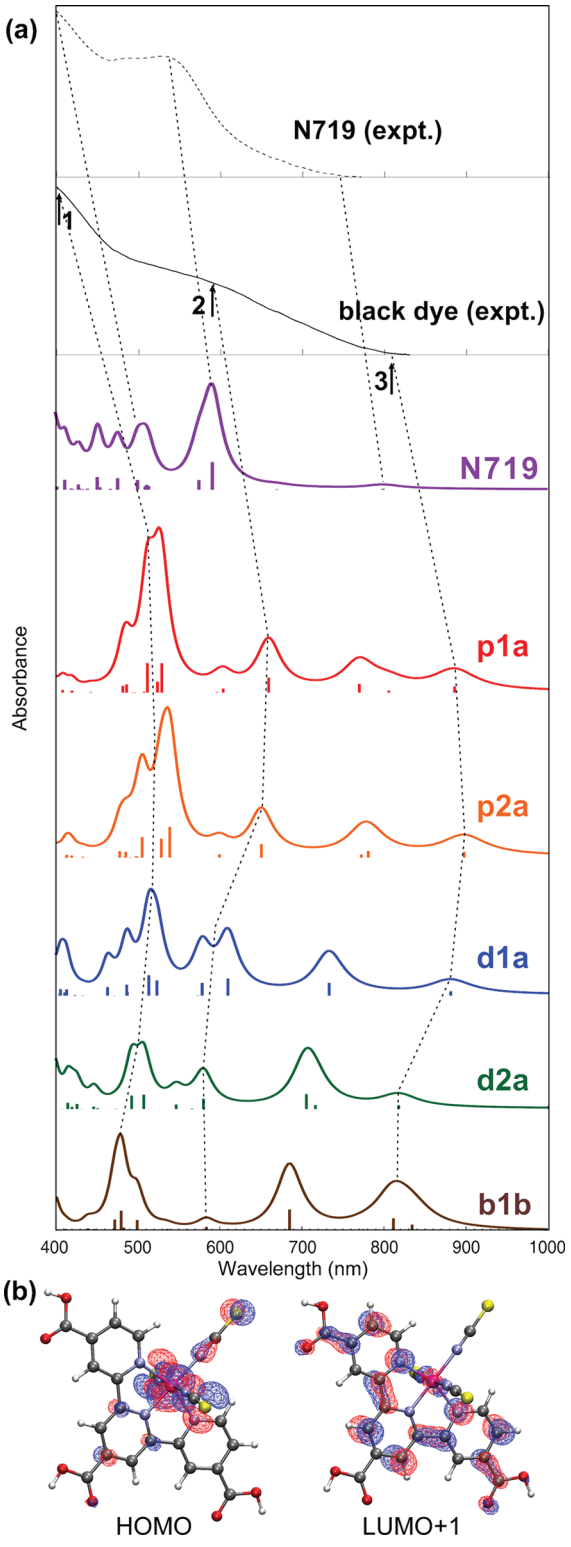

Figure 2. (a) UV−visible spectra of the black dye molecule of protonated one-anchor **p1a**, two-anchor **p2a**, deprotonated one-anchor **d1a**, two-anchor **d2a**, bidentate bridging one-anchor **b1b** structures, and N719 dye adsorbed structures calculated by TDDFT. Experimental spectra are shown for black dye (black solid line) and N719 dye (black dashed line) on the top of the figure. The six dotted vertical guide lines connect peaks 1 and 2 and the tail positions of the black dye and N719 dye, respectively. (b) Kohn−Sham orbitals of HOMO and LUMO+1, constituting the main configuration of the peak at 657 nm in the black dye **p1a** structure.

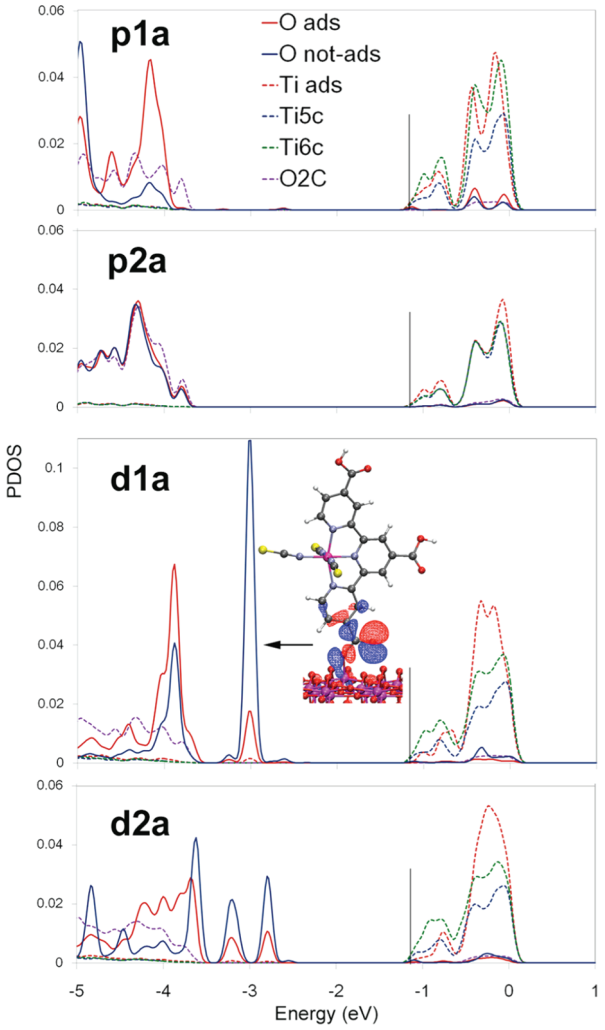

Figure 3. PDOSs of the protonated (**p1a**, **p2a**) and deprotonated (**d1a**, **d2a**) adsorbed structures of black dye on the TiO_2 anatase (101) surface. "O ads" ("O not-ads") represents the adsorbed (not adsorbed) oxygen atom of the anchor carboxyl group. "Ti ads" represents the adsorbed Ti atom. The black vertical line represents the HOMO energy of the whole system. The Kohn−Sham orbital of the gap state in **d1a** is also shown.

problem in the metal complex with charge-transfer-type excitations.[31] In the experimental spectra, black dye has a strong peak 1 (~410 nm) near the N719 peak 1 (~410 nm) and another peak 2 (~600 nm) at a longer wavelength compared to the N719 peak 2 (~540 nm). The most important feature of black dye is the tail position at a longer wavelength in the near-IR region than that of N719. Here, we regard the lowest-energy maxima indicated by tail 3 in the UV−visible spectra (Figure 2a) as the tail position. On the basis of this tail position, the structures **d2a** and **b1b** are excluded because there is no shift compared to that in the N719. In the spectrum of **d1a**, we found a narrower gap between peaks 1 and 2. Thus, this structure can be excluded as well. Consequently, the spectra of **p1a** and **p2a** are found to be most consistent with the experimental spectra. Note that it is difficult to distinguish between these protonated structures at the level of present accuracy.

It is meaningful to assign the electronic configurations related to the two main peaks in black dye. In the **p1a** spectrum, peak 1, around 520 nm, consists of HOMO−1 → LUMO+2 and

dx.doi.org/10.1021/jz201583n | J. Phys. Chem.Lett. 2012, 3, 472−477

HOMO−3 → LUMO contributions, while HOMO → LUMO +1 is responsible for the peak at 657 nm. These HOMOs are mainly constructed from the NCS ligand nonbonding orbital as well as the ruthenium 4d orbital, while the LUMOs are the delocalized π^* orbitals on the terpyridyl ligand. Figure 2b shows the orbital density of the HOMO and LUMO+1 for peak 2. As proposed in the black dye and N719 cases, Ru dyes have ligand−ligand excitations with some overlap of the initial and final orbitals at the Ru site.[32,33] This is an advantage of Ru dyes that gives better charge separation to prevent intramolecular recombination with reasonable oscillator strength. Note that the calculated HOMO → LUMO excitation (at 767 nm) has a weak intensity; therefore, the question of HOMO and LUMO positions is not relevant. (Detailed data of TDDFT calculations are listed in Supporting Information Figure S3 and Table S1.)

Returning to the dye/TiO_2 surface systems, we investigated the relationship between the protonation and deprotonation by using PDOS. Figure 3 shows the PDOSs of **p*n*a** and **d*n*a**. In the PDOS of **d1a**, one gap state appears, which is localized at two oxygen atoms in the carboxylate group anchor. This is because the negative charge of the carboxylate pushes up the oxygen 2p states. Two gap states in the PDOS of **d2a** have the same characters. We also found an increase of PDOS at the adsorbed Ti sites in the conduction band. This can be also attributed to the negativity of the carboxylate anchor. On the other hand, there is no such change in the cases with the protonated carboxyl anchors because of their neutrality. We conclude that the charge of the carboxyl anchor is more responsible for the electronic states of the adsorption site than the proton adsorbed at a surface site.

In summary, we have investigated the stability of possible adsorption modes of Ru N749 dye (black dye) on a TiO_2 anatase (101) surface with DFT calculations with the periodic boundary condition. We found that the protonated carboxyl mode is more stable than the deprotonated, and the single protonated carboxyl anchor is the most stable. This stability is mainly attributed to the formation of a HB between the proton in the carboxyl anchor and the surface O_{2c} site. The present stability is confirmed by the comparison of UV−visible spectra between our calculations and experiments; the protonated anchor modes give more consistency. Although inclusion of solvent into the calculations[34,35] might make some modifications, this concept of the stable protonated carboxyl anchor gives a novel perspective to the anchoring mechanism of Ru polypyridyl dye complexes to the TiO_2 surfaces and a fundamental starting point for improving the efficiency of DSC.

COMPUTATIONAL DETAILS

We carried out geometry optimizations of the surface−dye systems at the level of DFT/BLYP and calculated the UV−visible spectra of dyes at the level of TDDFT/B3LYP. DFT-based geometry optimizations of black dye on the TiO_2 anatase (101) surface were carried out with the CPMD code.[36] We used the supercell approach with the periodic boundary condition and plane wave basis set (cutoff energy = 70 Ry) with a Troullier−Martin type pseudopotential to avoid any artifacts of cluster models for the surface and any dependence of the local basis sets for the delocalized nature of electrons on the surface. The unit cell has a = 22.7052 Å, b = 20.47904 Å, c = 34.05780 Å, and α = 111.689°, where a, b, c, and α correspond to the experimental lattice parameters (Supporting Information Figure S1). This supercell involves the 6 × 2 TiO_2 anatase (101) surface with two layers leading to the $(TiO_2)_{96}$ composition, the vacuum region with 30 Å thickness, and the one black dye. Because black dye intrinsically has −1 charge, we use this charge for the supercell calculations with a compensating homogeneous background. To take into account the flexibility of the adsorption angle, we carried out preliminary DFT-based molecular dynamics to prepare several initial structures for the geometry optimizations. From the viewpoint of the computational cost and the accuracy, the BLYP functional was used in this stage. Analysis of PDOS was carried out based on these optimized surface systems afterward. We carried out TDDFT linear response calculations with the cluster boundary condition and CPCM to mimic the acetonitrile solution environment, using the Gaussian09 package.[37] We used the B3LYP hybrid functional for higher accuracy. The functional dependence is discussed in Supporting Information Table S2. In order to cover a wider range of wavelengths, we adopted 250 excited states.

ASSOCIATED CONTENT

Supporting Information

Description of the computational details; geometry optimization when the proton is located at the O_{2c} nearest to the anchoring site; Kohn−Sham orbitals of the black dye molecule in the **p1a** structure; assignment of the UV−visible spectrum peaks of **p1a**, **p2a**, **d1a**, **d2a**, and **b1b** structures of black dye; and validity of the BLYP functional. This material is available free of charge via the Internet at http://pubs.acs.org.

AUTHOR INFORMATION

Corresponding Author

*E-mail: TATEYAMA.Yoshitaka@nims.go.jp.

ACKNOWLEDGMENTS

This work was partly supported by KAKENHI 20540384 and 23340089 as well as the Strategic Programs for Innovative Research (SPIRE), MEXT and the Computational Materials Science Initiative (CMSI), Japan. The calculation was carried out on the supercomputer center in the ISSP, The University of Tokyo, T2K-Tokyo, T2K-Tsukuba and NIMS. We thank Prof. Jaroslav Burda and Mr. Zudenek Futera for giving us the Ru ECP with f-type function basis sets.

REFERENCES

(1) O'Regan, B.; Grätzel, M. A low-Cost, High-Efficiency Solar Cell Based on Dye-Sensitized Colloidal TiO_2 Films. *Nature* **1991**, *353*, 737−740.

(2) Grätzel, M. Photoelectrochemical Cells. *Nature* **2001**, *414*, 338−344.

(3) Hagfeldt, A.; Boschloo, G.; Sun, L.; Kloo, L.; Pettersson, H. Dye-Sensitized Solar Cells. *Chem. Rev.* **2010**, *110*, 6595−6663.

(4) Nazeeruddin, M. K.; Kay, A.; Rodicio, I.; Humphry-Baker, R.; Müller, E.; Liska, P.; Vlachopoulos, N.; Grätzel, M. Conversion of Light to Electricity by *cis*-X_2Bis(2,2′-bipyridyl-4,4′-decarboxylate)-ruthenium(II) Charge-Transfer Sensitizers (X = Cl^-, Br^-, I^-, CN^-, and SCN^-) on Nanocrystalline TiO_2 Electrodes. *J. Am. Chem. Soc.* **1993**, *115*, 6382−6390.

(5) Nazeeruddin, M. K.; Zakeeruddin, S. M.; Humphry-Baker, R.; Jirousek, M.; Liska, P.; Vlachopoulos, N.; Shklover, V.; Fischer, C.; Grätzel, M. Acid−Base Equilibria of (2,2′-Bipyridyl-4,4′-dicarboxylic acid)ruthenium(II) Complexes and the Effect of Protonation on Charge-Transfer Sensitization of Nanocrystalline Titania. *Inorg. Chem.* **1999**, *38*, 6298−6305.

(6) Nazeeruddin, M. K.; Péchy, P.; Renouard, T.; Zakeeruddin, S. M.; Humphry-Baker, R.; Comte, P.; Liska, P.; Cevey, L.; Costa, E.; Shklover, V.; et al. Engineering of Efficient Panchromatic Sensitizers for Nanocrystalline TiO_2-Based Solar Cells. *J. Am. Chem. Soc.* **2001**, *123*, 1613−1624.
(7) Chiba, Y.; Islam, A.; Watanabe, Y.; Komiya, R.; Koide, N.; Han, L. Dye-Sensitized Solar Cells with Conversion Efficiency of 11.1%. *Jpn. J. Appl. Phys.* **2006**, *45*, L638−L640.
(8) Hara, K.; Kurashige, M.; Dan-oh, Y.; Kasada, C.; Shinpo, A.; Suga, S.; Sayama, K.; Arakawa, H. Design of New Coumarin Dyes Having Thiophene Moieties for Highly Efficient Organic-Dye-Sensitized Solar Cells. *New J. Chem.* **2003**, *27*, 783−785.
(9) Hara, K.; Sato, T.; Katoh, R.; Furube, A; Yoshihara, T.; Murai, M.; Kurashige, M.; Ito, S.; Shinpo, A.; Suga, S.; et al. Novel Conjugated Organic Dyes for Efficient Dye-Sensitized Solar Cells. *Adv. Funct. Mater.* **2005**, *15*, 246−252.
(10) Yella, A.; Lee, H.-W.; Tsao, H. N.; Yi, C.; Chandiran, A. K.; Nazeeruddin, M. K.; Diau, E. W.-G.; Yeh, C.-Y.; Zakeeruddin, S. M.; Grätzel, M. Porphyrin-Sensitized Solar Cells with Cobalt (II/III)-Based Redox Electrolyte Exceed 12% Efficiency. *Science* **2011**, *334*, 629−634.
(11) Meng, S.; Ren, J.; Kaxiras, E. Natural Dyes Adsorbed on TiO_2 Nanowire for Photovoltaic Applications: Enhanced Light Absorption and Ultrafast Electron Injection. *Nano Lett.* **2008**, *8*, 3266−3272.
(12) De Angelis, F.; Fantacci, S.; Selloni, A.; Nazeeruddin, M. K.; Grätzel, M. First-Principles Modeling of the Adsorption Geometry and Electronic Structure of Ru(II) Dyes on Extended TiO_2 Substrates for Dye-Sensitized Solar Cell Applications. *J. Phys. Chem. C* **2010**, *114*, 6054−6061.
(13) Bauer, C.; Boschloo, G.; Mukhtar, E.; Hagfeldt, A. Interfacial Electron-Transfer Dynamics in Ru(tcterpy)$(NCS)_3$-Sensitized TiO_2 Nanocrystalline Solar Cells. *J. Phys. Chem. B* **2002**, *106*, 12693−12704.
(14) Duncan, W. R.; Stier, W. M.; Prezhdo, O. V. Ab Initio Nonadiabatic Molecular Dynamics of the Ultrafast Electron Injection across the Alizarin−TiO_2 Interface. *J. Am. Chem. Soc.* **2005**, *127*, 7941−7951.
(15) Finnie, K. S.; Bartlett, J. R.; Woolfrey, J. L. Vibrational Spectroscopic Study of the Coordination of (2,2′-Bipyridyl-4,4′-dicarboxylic acid)ruthenium(II) Complexes to the Surface of Nanocrystalline Titania. *Langmuir* **1998**, *14*, 2744−2749.
(16) Nazeeruddin, M. K.; Humphry-Baker, R.; Liska, P.; Grätzel, M. Investigation of Sensitizer Adsorption and the Influence of Protons on Current and Voltage of a Dye-Sensitized Nanocrystalline TiO_2 Solar Cell. *J. Phys. Chem. B* **2003**, *107*, 8981−8987.
(17) Fantacci, S.; De Angelis, F. A Computational Approach to the Electronic and Optical Properties of Ru(II) and Ir(III) Polypyridyl Complexes: Applications to DSC, OLED and NLO. *Coord. Chem. Rev.* **2011**, *255*, 2704−2726.
(18) Persson, P.; Lundqvist, M. J. Calculated Structural and Electronic Interactions of the Ruthenium Dye N3 with a Titanium Dioxide Nanocrystal. *J. Phys. Chem. B* **2005**, *109*, 11918−11924.
(19) De Angelis, F.; Fantacci, S.; Selloni, A.; Nazeeruddin, M. K.; Grätzel, M. Time-Dependent Density Functional Theory Investigations on the Excited States of Ru(II)-Dye-Sensitized TiO_2 Nanoparticles: The Role of Sensitizer Protonation. *J. Am. Chem. Soc.* **2007**, *129*, 14156−14157.
(20) De Angelis, F.; Fantacci, S.; Selloni, A.; Grätzel, M.; Nazeeruddin, M. K. Influence of the Sensitizer Adsorption Mode on the Open-Circuit Potential of Dye-Sensitized Solar Cells. *Nano Lett.* **2007**, *7*, 3189−3195.
(21) De Angelis, F.; Fantacci, S.; Selloni, A.; Grätzel, M.; Nazeeruddin, M. K. Alignment of the Dye'S Molecular Levels with the TiO_2 Band Edges in Dye-Sensitized Solar Cells: A DFT-TDDFT Study. *Nanotechnology* **2008**, *19*, 424002.
(22) De Angelis, F.; Fantacci, S.; Mosconi, E.; Nazeeruddin, M. K.; Grätzel, M. Absorption Spectra and Excited State Energy Levels of the N719 Dye on TiO_2 in Dye-Sensitized Solar Cell Models. *J. Phys. Chem. C* **2011**, *115*, 8825−8831.
(23) Schiffmann, F.; VandeVondele, J.; Hutter, J.; Wirz, R.; Urakawa, A.; Baiker, A. Protonation-Dependent Binding of Ruthenium Bipyridyl Complexes to the Anatase(101) Surface. *J. Phys. Chem. C* **2010**, *114*, 8394−8404.
(24) Vittadini, A; Selloni, A; Rotzinger, F. P.; Grätzel, M. Formic Acid Adsorption on Dry and Hydrated TiO_2 Anatase (101) Surfaces by DFT Calculations. *J. Phys. Chem. B* **2000**, *104*, 1300−1306.
(25) Szieberth, D.; Ferrari, A. M.; Dong, X. Adsorption of Glycine on the Anatase (101) Surface: An Ab Initio Study. *Phys. Chem. Chem. Phys.* **2010**, *12*, 11033−11040.
(26) Martin, R. M. *Electronic Structure*; Cambridge University Press: Cambridge, U.K., 2004.
(27) Marques, M. A. L.; Ullrich, C. A.; Nogueira, F.; Rubio, A.; Burke, K.; Gross, E. K. U. *Time-Dependent Density Functional Theory*; Springer: Berlin, Germany, 2006.
(28) Izutsu, K. *Electrochemistry in Nonaqueous Solutions*; Wiley-VCH: Weinheim, Germany, 2009.
(29) Sumita, M.; Hu, C.; Tateyama, Y. Interface Water on TiO_2 Anatase (101) and (001) Surfaces: First-Principles Study with TiO_2 Slabs Dipped in Bulk Water. *J. Phys. Chem. C* **2010**, *114*, 18529−18537.
(30) Cheng, J.; Sprik, M. Acidity of the Aqueous Rutile TiO_2(110) Surface from Density Functional Theory Based Molecular Dynamics. *J. Chem. Theory Comput.* **2010**, *6*, 880−889.
(31) Cramer, C. J.; Truhlar, D. G. Density Functional Theory for Transition Metals and Transition Metal Chemistry. *Phys. Chem. Chem. Phys.* **2009**, *11*, 10757−10816.
(32) Aiga, F.; Tada, T. Molecular and Electronic Structures of Black Dye; An Efficient Sensitizing Dye for Nanocrystalline TiO_2 Solar Cells. *J. Mol. Struct.* **2003**, *658*, 25−32.
(33) Nazeeruddin, M. K.; De Angelis, F.; Fantacci, S.; Selloni, A.; Viscardi, G.; Liska, P.; Ito, S.; Takeru, B.; Grätzel, M. Combined Experimental and DFT-TDDFT Computational Study of Photoelectrochemical Cell Ruthenium Sensitizers. *J. Am. Chem. Soc.* **2005**, *127*, 16835−16847.
(34) Schiffmann, F.; VandeVondele, J.; Hutter, J.; Urakawa, A.; Wirz, R.; Baiker, A. An Atomistic Picture of the Regeneration Process in Dye Sensitized Solar Cells. *Proc. Natl. Acad. Sci. U.S.A.* **2010**, *107*, 4830−4833.
(35) Sumita, M.; Sodeyama, K.; Han, L.; Tateyama, Y. Water Contamination Effect on Liquid Acetonitrile/TiO_2 Anatase (101) Interface for Durable Dye-Sensitized Solar Cell. *J. Phys. Chem. C* **2011**, *115*, 19848−19855.
(36) *CPMD V3.12*. IBM Research division, MPI Festkoerperforschung, Stuttgart, Germany; http://www.cpmd.org (2012).
(37) Frish, M. J. et al. *GAUSSIAN 09*, revision A.02; Gaussian, Inc.: Wallingford, CT, 2004.